HHS Public Access

Author manuscript

Nature. Author manuscript; available in PMC 2014 August 27.

Published in final edited form as:

Nature. 2014 February 27; 506(7489): 503–506. doi:10.1038/nature12902.

Sessile alveolar macrophages modulate immunity through connexin 43-based epithelial communication

Kristin Westphalen[1], **Galina A. Gusarova**[1], **Mohammad N. Islam**[1], **Manikandan Subramanian**[2], **Taylor S. Cohen**[3], **Alice S. Prince**[3], and **Jahar Bhattacharya**[1,4]

[1]Lung Biology Laboratory, Department of Medicine, Division of Pulmonary, Allergy and Critical Care, College of Physicians and Surgeons, Columbia University Medical Center, New York, New York, USA

[2]Department of Medicine, Division of Molecular Medicine, College of Physicians and Surgeons, Columbia University Medical Center, New York, New York, USA

[3]Department of Pediatrics, College of Physicians and Surgeons, Columbia University Medical Center, New York, New York, USA

[4]Department of Physiology & Cellular Biophysics, College of Physicians and Surgeons, Columbia University Medical Center, New York, New York, USA

Abstract

Tissue-resident macrophages of barrier organs constitute the first line of defense against pathogens at the systemic interface with the ambient environment. In lung, resident alveolar macrophages (AMs) provide sentinel function against inhaled pathogens[1]. Bacterial constituents ligate toll-like receptors (TLRs) on AMs[2], causing AMs to secrete proinflammatory cytokines[3] that activate alveolar epithelial receptors[4], leading to recruitment of neutrophils that engulf pathogens[5,6]. However, since the AM-induced immune response could itself cause tissue injury, it is unclear how AMs modulate the response to prevent injury. Here, through real-time alveolar imaging *in situ*, we show that a subset of AMs attached to the alveolar wall, formed connexin 43 (Cx43)-containing gap junctional channels (GJCs) with the epithelium. During lipopolysaccharide (LPS)-induced inflammation, the AMs remained alveolus-attached and sessile, and they established intercommunication through synchronized Ca^{2+} waves, using the epithelium as the conducting pathway. The intercommunication was immunosuppressive, involving Ca^{2+} dependent activation of Akt, since AM-specific knockout of Cx43 enhanced alveolar neutrophil recruitment and secretion of proinflammatory cytokines in the bronchoalveolar lavage (BAL). The picture emerges

Correspondence and requests for materials should be addressed to J.B. (jb39@columbia.edu).

Supplementary Information is linked to the online version of the paper at www.nature.com/nature

Author Contributions K.W. designed and carried out the experiments, prepared the figures and wrote the initial manuscript. G.A.G contributed to Western Blot, Immunoprecipitation and FRAP experiments. M.N.I. carried out the NFκB *in situ* stainings, contributed to BAL cell counting and survival studies. M.S. performed the antigen presentation assay and provided the CD11cMyD88$^{-/-}$ mice. T.S.C. provided *S. aureus* and contributed to ELISA studies. A.P. contributed to the experimental design. J.B. was responsible for the overall project, designed the experiments and wrote the initial manuscript. All authors edited the manuscript.

The authors declare no competing financial interests.

of a novel immunomodulatory process in which a subset of alveolus-attached AMs intercommunicates immunosuppressive signals to reduce endotoxin-induced lung inflammation.

Since most of our understanding of AMs is based on studies in which AMs were isolated by bronchoalveolar lavage (BAL) and studied *in vitro*, or in which they were depleted from the lungs[5,7], we lack understanding of dynamic interactions between AMs and the alveolar epithelium that might critically modulate the lung's inflammatory response. To determine these interactions *in situ*, we took advantage of the fact that AMs express CD11c[8] and crossed CD11c-cre mice[9] with Rosa26-LSL-EYFP mice[10] to obtain mice expressing enhanced yellow fluorescence protein (YFP) in CD11c-expressing cells.

Live confocal microscopy of isolated, blood-perfused mouse lungs[11] derived from CD11c/EYFP mice revealed YFP positive (YFP^+) cells in the subpleural interstitium and the alveolar lumen (Fig. 1a). To distinguish AMs from lung dendritic cells (DCs) that also express CD11c[8,12], we gave intra-alveolar microinjections of the AM marker, Siglec F[13], and an antibody for the major histocompatibility complex class II (MHC-II), which marks lung DCs[12]. These microinjections revealed that luminal YFP^+ cells were AMs, since they stained strongly for Siglec F, but weakly for MHC-II (Fig. 1b) whereas interstitial YFP^+ cells that we stained by topical antibody-applications to the saponin-permeabilized pleura were MHC-II^+/Siglec F^- DCs (Fig. 1b). The alveolar epithelium inhibits trans-epithelial transit of reagents injected in the alveolar lumen[4]. Hence, alveolar microinjections of dye resulted in fluorescence uptake in AMs, but not in DCs (Fig. 1c), suggesting that DCs did not communicate with the alveolar lumen. In further affirmation that luminal YFP^+ cells were AMs, YFP^+-MHC-II^{low} cells recovered in the BAL failed to induce T cell proliferation in antigen-presentation assays (Extended Data Fig. 1a). Together, these findings indicate that YFP^+ AMs localized to the alveolar lumen, while YFP^+ DCs were compartmentalized in the perialveolar interstitium.

We detected a single AM for approximately every 3 alveoli (Extended Data Fig. 1b), suggesting that AMs carry out pathogen surveillance by patrolling the alveolar surface[14]. However contrary to this expectation, AMs remained stationary at fixed alveolar locations for the duration of our imaging studies lasting up to 4 h (Extended Data Fig. 1c). Our attempts at dislodging AMs by BAL or by direct alveolar microinjection of buffer were unsuccessful (Extended Data Fig. 1c). To determine whether AMs might be induced to migrate towards bacteria, we microinjected *Staphylococcus aureus* (*S. aureus*) in the alveolar lumen. Although AMs rapidly ingested *S. aureus* that lay within one AM diameter, they did not migrate towards bacteria (Fig.1d, Extended Data Fig. 1c). The alveolar liquid flow[15] appeared to wash bacteria towards AMs (not shown). Thus, contrary to expectation, our findings indicate that AMs were sessile.

Macrophages express connexin 43 (Cx43)[16], potentially enabling AMs to form GJCs with the alveolar epithelium. To determine GJCs, we applied photolytic uncaging to induce cell-specific increases of cytosolic Ca^{2+} [17], and fluorescence recovery after photobleaching (FRAP) to quantify intercellular dye diffusion[11]. In 40% of AMs, uncaging-induced Ca^{2+} waves travelled from the epithelium to AMs (Fig. 1e) and in the opposite direction (not shown). Cx43 expression in AMs correlated directly with FRAP (Fig. 1f). A one-hour

treatment with GAP 26/27, an inhibitor of Cx43-based GJCs and hemichannels, blocked uncaging-induced Ca^{2+} waves (Fig. 1e) as well as FRAP (not shown) between AMs and the epithelium. In $CD11c^{high}$-MHC-II^{low} AMs, which we obtained respectively, by BAL and by extraction from lung tissue after BAL (Extended Data Fig. 1a,d), Cx43 protein and mRNA expressions were higher in tissue than BAL AMs (Fig. 1g), suggesting that Cx43 was higher in alveolus-adherent than –non-adherent AMs. In mice with CD11c-specific *Cx43* knockout ($CD11cCx43^{-/-}$) (Extended Data Fig.2a), AMs remained immobile even after alveolar microinjections of bacteria or PBS (Extended Data Fig. 2b,c). Hence, Cx43 was not responsible for AM immobility. In lungs given intranasal *Escherichia coli*-derived LPS instillation, neutrophils entered and migrated freely on the alveolar surface (Supp. Fig. 1, Supp. Video 1), ruling out non-specific physical factors in causing AM immobility. Taken together, our findings reveal the presence of $Cx43^{high}$ and $Cx43^{low}$ AM populations in the lung, in which $Cx43^{high}$ AMs formed GJCs with the alveolar epithelium.

To induce lung injury, we gave mice intranasal LPS, or PBS (control). We removed lungs 1, 4 or 24 h after the instillations to establish IPLs for imaging studies[11]. Instillation of fluorescent LPS confirmed LPS entry in AMs (Fig. 2a). Fluorescent LPS did not enter interstitial DCs, indicating that in alveoli LPS ligated AMs, not DCs. Fluorescent LPS uptake was markedly greater in BAL-derived DCs than in DCs recovered from the tissue of post-lavage lungs, suggesting that access to the airway lumen maybe greater for BAL- than tissue-derived DCs (Extended Data Fig. 3).

In contrast to PBS-treated lungs in which there were no notable effects, AMs of LPS-treated lungs displayed synchronous Ca^{2+} spikes that occurred within 1 min in AM clusters. Spikes lasted 10–15 s, appearing every 10–20 min (Fig. 2b, Supp. Video 2). They initiated 4 h after LPS and increased over 24 h (Fig. 2c). Concomitant Ca^{2+} spikes occurred in the adjoining epithelium (Fig. 2d). The spikes travelled between different AMs, often separated by 8 alveoli, across the intervening epithelium (Fig. 2b and Extended Data Fig. 4a). We did not identify a specific"pacemaker" AM that initiated synchronous spiking. Intra-alveolar microinjection of GAP 26/27 blocked synchronous epithelial and AM spikes (Fig. 2d,e), suggesting interdependence between these responses. GAP26/27 did not block non-synchronous spikes (not shown). Connexin hemichannels are implicated in some forms of ATP dependent purinergic signaling[18]. However after LPS treatment, cytosolic dyes (fluo-4, calcein) that can transit connexin channels did not leak from AMs or the epithelium (Extended Data Fig. 4b,c). The ATP receptor inhibitor, pyridoxal phosphate-6-azo(benzene-2,4-disulfonic acid) tetrasodium salt hydrate (PPADS) did not modify spike formation (Fig. 2e). These findings rule out a role for connexin hemichannels in inducing spike intercommunication. Alveolar microinfusion of the inositol-(1,4,5)-triphosphate (InsP3) receptor inhibitor, xestospongin C, but not depletion of extracellular Ca^{2+}, blocked the Ca^{2+} spikes (Fig. 2e), indicating that the spikes resulted from Ca^{2+} release from intracellular stores. Depletion of alveolar neutrophils, which we identified as $CD11b^{+}$ cells of 6–8 μm diameter, did not diminish spike formation (Extended Data Fig. 4d). The numbers of AMs per imaging field were identical at all time points (Extended Data Fig. 4e). Together, these findings indicate that LPS induced intercommunicated Ca^{2+} spikes between AMs lying in different alveoli and that the communication occurred through the epithelium.

LPS ligation of TLR4 induces signaling through the adapter proteins, myeloid differentiation factor 88 (MyD88) and the TIR-domain-containing adapter-inducing interferon-β (TRIF)[19]. MyD88 and TRIF are implicated in lung injury[20,21]. We generated mice (CD11cMyD88$^{-/-}$) lacking *MyD88* in CD11c-expressing cells[22]. In CD11cMyD88$^{-/-}$, but not WT mice, LPS-induced Ca^{2+} spikes in AMs (Fig. 3a) and the epithelium (Fig. 3b,c) were lacking, and alveolar neutrophil entry at 24h was diminished (Fig. 3d,e), although both mice had similar Cx43 expression in AMs (Extended Data Fig. 4f). We conclude that MyD88-dependent signaling was responsible for the LPS-induced spike formation and lung inflammation, and that AMs initiated the signaling.

Synchronous spikes in AMs and the epithelium were inhibited in CD11cCx43$^{-/-}$ mice (Fig. 3a-c), although non-synchronous Ca^{2+} spikes in AMs were similar to that of WT mice (Fig. 3a). Lung inflammation was markedly greater in CD11cCx43$^{-/-}$ than WT mice, as indicated by increased LPS- or *E.coli*-induced alveolar neutrophil recruitment and BAL leukocyte counts (Fig. 3d,e, Extended Data Fig. 5). As compared with Cx43$^{floxed/floxed}$ mice (littermate controls), BAL from CD11cCx43$^{-/-}$ mice contained more proinflammatory cytokines (Fig. 4a). Cx43 knockdown in bone marrow-derived macrophages did not alter cytokine secretion (Extended Data Fig. 6), ruling out Cx43 depletion as a determinant of the response. LPS-induced mortality was higher in CD11cCx43$^{-/-}$ mice than in littermate controls (Fig. 4b). In CD11cCx43$^{-/-}$ mice LPS caused greater degradation of IκBα (Fig. 4c) and increased nuclear translocation of NFκB (Extended Data Fig. 7a). AM numbers did not differ between WT and CD11cCx43$^{-/-}$ mice (Extended Data Fig. 7b). Together, these findings indicate that Cx43 knockout in AMs augmented LPS-induced inflammation and lung injury, indicating AM-epithelium GJCs were protective.

Increase of intracellular Ca^{2+} activates the Ca^{2+}/calmodulin-dependent kinase kinase (CAMKK) and its downstream target, the pro-survival kinase Akt[23,24]. Since these mechanisms are undetermined for lung inflammation, we immunoprecipitated CAMKKα or Akt from WT lungs. In each case, LPS enhanced pull-down of the corresponding binding partner (Fig. 4d), and it enhanced Akt phosphorylation in WT, but not in CD11cCx43$^{-/-}$ mice (Fig. 4c). Imaging indicated that the alveolar epithelium was the site of the LPS-induced enhancement of phospho-Akt expression (Fig. 4e). This effect was inhibited in CD11cCx43$^{-/-}$ mice (Fig. 4e) and by treatment with the intracellular Ca^{2+} chelator BAPTA-AM (Extended Data Fig. 8a). siRNA-induced knockdown of CAMKKα decreased Akt phosphorylation, while increasing IκBα degradation and BAL leukocyte counts (Fig. 4f,g). We generated SPC-Cx43$^{-/-}$ mice lacking *Cx43* in the alveolar epithelium[25]. In SPC-Cx43$^{-/-}$ mice, LPS-induced responses were similar to those of CD11cCx43$^{-/-}$ mice in that Akt phosphorylation decreased and BAL leukocyte counts increased (Extended Data Fig. 8b). Thus, loss of Cx43 on either face of AM-epithelial GJCs induced similar effects. These findings indicate that Cx43-based AM GJCs suppressed inflammation through CAMKKα-induced phosphorylation of epithelial Akt.

In conclusion, our studies highlight the importance of intercellular connectivity in lung immunity. AMs critically elicit lung inflammation. However concomitantly, sets of alveolus-attached AMs intercommunicate immunosuppressive signals. Cx43 deletion in AMs increased secretion of cytokines that were likely to be predominantly of AM (MIP-1α)

and of epithelial (CXCL1,5) origin, suggesting the possibility that AMs and the epithelium might mutually suppress cytokine release. Previous lung studies implicated syncytial connectivity in endothelium and epithelium in surfactant secretion[17], leukocyte recruitment[26] and hypoxic vasoconstriction[27]. Here we show that Cx43^{high} AMs co-opt the syncytial communication to subvert lung inflammation. This communication might play a role in other forms of lung inflammation such as those involving tolerogenic responses to antigen. Although future studies are needed to further elucidate the roles of Ca^{2+}-regulatory mechanisms in this process, especially regarding second messengers such as InsP3 that can diffuse through GJCs[28], we propose that Cx43 expression in AMs might provide a drug-delivery focus for therapy of inflammatory lung disease.

METHODS SUMMARY

All animal experiments were approved by the Institutional Animal Care and Use Committee of Columbia University Medical Center. We imaged isolated, blood-perfused lungs by laser scanning microscopy (LSM 510 META, Zeiss)[11]. Alveoli were imaged to a depth of 40 μm from the pleura. We loaded alveolar cells with dyes and reagents by alveolar micropuncture[11]. LPS concentrations were 1 mg (kg body weight)$^{-1}$ for all experiments, and 25 mg kg^{-1} for survival studies. We infused calcein-stained *S. aureus* (1x10^8 bacteria ml^{-1}) by alveolar micropuncture. For Ca^{2+} imaging (1 image 5s^{-1}), we microinfused alveoli with fluo-4. For photolytic Ca^{2+} uncaging[17], we targeted single cells, co-loaded with fluo-4 and the UV-sensitive Ca^{2+} cage, *o*-Nitrophenyl EGTA, with high intensity UV illumination (~320 nm, 10 pulses s^{-1}) in 2-μm diameter spots. *In situ* Cx43, NFκB and Akt staining was carried out after fixation and permeabilization of the alveolus. We quantified Cx43 mRNA by qPCR in AMs sorted from BAL and lung tissue samples (Influx Cell Sorter, BD Biosciences). BAL and cell culture supernatant cytokines were analyzed by ELISA. Western Blot analyses and Co-immunoprecipitations were performed as previously described[29]. siRNA was complexed with freshly extruded liposomes and intranasally instilled.

METHODS

Fluorophores

We purchased fluo-4 AM, calcein AM, calcein red AM and TO-PRO-3 Iodide (642/661) from Invitrogen.

Antibodies

We purchased fluorescence tagged antibodies against CD11c (Cat. # 11-0114), MHC-II (Cat. # 17-5321), CD11b (Cat. # 12-0112, Cat. # 17-0112), CD4 (Cat. # 11-0043-85), CD8 (Cat. # 17-0081-81), CD3 (Cat. # 17-0032-82) and Ly6G (Cat. # 12-5931) from eBiosciences; Alexa Fluor 633 goat anti-rabbit IgG antibody (Cat. # A-21071) and Alexa Fluor 488 goat anti-rabbit IgG antibody (Cat. # A-11008) from Invitrogen and Siglec F antibody (Cat.# 552126) from BD Pharmingen. Appropriate IgG controls were purchased from eBiosciences. We purchased IκBα antibody (Cat. # sc-371-G), NFκB p65 antibody (Cat. # sc-109), Cx43 antibody (Cat. # sc-9059) and CAMKKα antibody (Cat. # sc-11370) from Santa Cruz Biotechnology and phospho-Akt (Thr308) (Cat. # 2965), Akt (pan) (Cat. #

4691), Cx43 antibody (Cat. # 3512) from Cell Signaling. As secondary antibodies for Western Blot, we purchased goat anti-rabbit IgG-HRP (Cat. # sc-2030), donkey anti-goat IgG-HRP (Cat. # sc-2033) from Santa Cruz.

Reagents

We purchased *o*-Nitrophenyl EGTA (NP-EGTA) (100 μM) and BAPTA (100 μM) from Invitrogen, Gap 27 (500 μM) from Tocris, Gap 26 (200 μM) from Alpha Diagnostics, xestospongin C (25 μM) from Calbiochem, Saponin (0.01 %) from ICN Biomedicals, Tween 20 (0.5%) from BIO-RAD and LPS (E.coli 0111:B4), fluorescent LPS (E.coli 0111:B4), Triton X-100 (0.2%), PPADS (100 μM), and doxycycline from Sigma. We purchased IL-6 ELISA kit from BioLegend and CXCL5 and MIP-1α ELISA kits from R&D systems.

Solutions

Agents were dissolved in HEPES-bufferend vehicle of pH 7.4 and osmolarity of 295 mOsm containing 150mM Na^+, 5mM K^+, 1mM Ca^{2+}, 1mM Mg^{2+} and 10 mM Glucose.

Animals

All animal procedures were approved by the Institutional Animal Care and Use Committee of Columbia University Medical Center. Animals were between 2–6 month old and age and sex-matched. All mice were on a C57BL/6 background, except Balb/c mice (Jackson Laboratory) that we used for antigen presentation assays and SPC-$Cx43^{-/-}$ mice, which were B6FVBF2. CD11c-cre mice were provided by Dr. Boris Reizis (Columbia University Medical Center, New York) and SPC-rtTA/TetO-Cre (SPC-Cre) mice were provided by Dr. Jeffrey Whitsett (Childrens Hospital Medical Center, Cincinnati), $Cx43^{floxed/floxed}$ (Stock # 008039) and C57BL/6 WT mice were purchased from Jackson Laboratory. To achieve pan-epithelial knockout of *Cx43* in SPC-$Cx43^{-/-}$ mice we maintained pregnant females on doxycycline (1mg/ml in drinking water) for 48h from embryonic (E) day E6.5–8.5[25]. Gestation was dated against day of vaginal plug formation.

ALI

We intranasally instilled LPS in sterile PBS at concentrations of 1mg (kg body weight)$^{-1}$ for all experiments, and 25 mg kg^{-1} for survival studies. We instilled control mice with PBS.

Bacteria

S. aureus LAC USA300[30] and *E. coli* (clinical isolate) grew on Luria-Bertani agar at 37 °C. For infection, we inoculated LB broth with a single colony that grew overnight at 37°C. We stained stationary phase *S. aureus* with Calcein (5 μM) and microinfused them at concentrations of 1×10^8 cells by alveolar micropuncture. *E. coli* was intranasally instilled at concentrations of 1×10^6 bacteria ml^{-1} in 1.5 ml PBS (kg body weight)$^{-1}$.

Lung imaging and *in situ* immunofluorescence

We used our previously reported methods to establish isolated blood-perfused mouse lungs for imaging experiments[11]. We imaged the lungs with a laser scanning microscopy system (LSM 510 META, Zeiss)[11]. All dyes and reagents were microinfused by alveolar

micropuncture[11]. In all experiments in which we infused more than 1 dye, we confirmed absence of bleed-through between fluorescence emission channels. We microinfused fluo-4 (10 μM) for 45 min, all other dyes (10 μM) and fluorescence tagged antibodies (4 μg ml^{-1}) for 20 min. Antibody infusions were followed by washout. For administrations through the permeabilized pleura, we topically applied Saponin (0.01 %) and then antibodies. We performed *in situ* staining for Cx43, NFκB and Akt after we fixed the lungs with paraformaldehyde (4%) for 20 min. After permeabilizing the alveolar epithelium with Tween 20 (0.5%) for Cx43 and Akt staining, or with Triton X-100 (0.2%) for NFκB staining, we blocked the tissue for 20 min with 1% fetal bovine serum (FBS) solution, then microinfused primary antibody (45 min) and secondary antibody (30 min) in 1 % FBS containing Hepes buffer. Nuclear staining was established with 1 μM TO-PRO-3 Iodide in solution with the secondary antibody. Each step was followed by a 15 min washout with Hepes buffer containing 1% FBS and 0.01% Tween 20. All images were recorded as single images and processed using MetaMorph imaging software or Image J. Brightness and contrast adjustments were applied to individual color channels of entire images and equally to all experimental groups. We did not apply further downstream processing or averaging.

Ca^{2+} determinations and uncaging

We detected cytosolic Ca^{2+} using fluo-4. We recorded Ca^{2+} responses at 1 image per every 5 or 10 s for 20 min. For photolytic Ca^{2+} uncaging, we loaded alveoli with fluo-4 and the UV-light sensitive Ca^{2+} cage, NP-EGTA. Then, we targeted a high intensity UV-beam (~320 nm, 10 pulses s^{-1} for 20–30s) that was 2 μm in diameter to single epithelial cells or AMs.

Cell isolation and immunofluorescence

We did all procedures on ice with Ca^{2+} free PBS containing 2 mM EDTA and 1% FBS, hereafter called “PBS”. Centrifugations were at 500 g for 5–10 min. To isolate BAL AMs, we lavaged 5 mice per experiment with 3×1 ml PBS. For lung tissue AM isolation, we perfused lungs with 5ml PBS through vascular cannulas to clear blood. We carefully passed lung tissue and spleens and through a 40 μm cell strainer (BD Biosciences). We stained splenic T cells with CD4 and CD8, splenic DCs with CD11c, and BAL and lung tissue AMs with CD11c and MHC-II antibodies. Incubations were for 1 h at a concentration of 2 μg ml^{-1}. We sorted the cells using an Influx Cell Sorter (BD Biosciences) or analyzed cells by flow cytometry (LSR II, BD Biosciences). We fixed and permeabilized AMs for Cx43 protein immunofluorescence. Cx43 or isotype specific IgG, and then secondary antibody incubations were for 1 h each, then we performed a cytospin (Thermo Scientific).

Antigen presentation assay

We assayed antigen presentation activity by mixed leukocyte reaction. We used lung AMs or splenic DC as antigen presenting cells and splenic T cells from C57BL/6 or Balb/c mice as responder cells. All cells were isolated by FACS-based sorting using specific antibodies. We confirmed cell viability of >95% as estimated by trypan blue dye (invitrogen) exclusion. We labeled splenic T cells with Cell Trace CFSE Proliferation Kit (Invitrogen). Per well of a 96 well plate, we incubated 15,000 T cells with 5,000 antigen presenting cells in DMEM

supplemented with 10% FBS, penicillin and streptomycin. Incubation of C57BL/6 T cells with isogenic splenic DCs served as negative control; Balb/c T cells with C57BL/6 splenic DCs served as positive control. C57BL/6 AMs from BAL were incubated with Balb/c T cells. After 3 days of co-culture, we measured T cell proliferation by CFSE dye dilution technique on $CD3^+$ gated cells by flow cytometry (FACScalibur, BD Biosciences). We set gating conditions of the flow cytometer using isotype- and fluorophore-matched IgGs. We analyzed primary data using standard software (FlowJO, Tree Star Inc.).

RNA extraction and quantitative RT-PCR

We extracted total RNA from 100–200,000 AMs per sample using the RNAqueous Micro Kit (Invitrogen). We converted equal amounts of RNA in cDNA using SuperScript III First-strand System for RT-PCR (Invitrogen). We performed TaqMan gene expression assays (Applied Biosystems, Carlsbad, CA) for Cx43 (Gja1, Mm00439105_m1) and for GAPDH as housekeeping gene. We performed PCRs in triplicates using an Applied Biosystems 7300 Real-Time PCR system. Data had identical cycle thresholds for GAPDH.

ELISA

We lavaged mice with 1ml Ca^{2+}-free PBS, centrifuged the samples at 500g for 15 min and preserved the supernatant for cytokine determinations. Sample testing was carried out by Quansys Biosciences using a multiplex chemiluminescence assay (Q-plex) for the detection of mouse cytokines and chemokines. ELISAs for IL-6, MIP-1a and CXCL5 were performed according to the manufacturer´s manual.

Immunoprecipitation

We cleared lungs from blood and BAL leukocytes by perfusion of the vasculature with 5 ml ice cold PBS and by BAL with 3x 1ml ice cold PBS. We then homogenized the lungs in IP Lysis buffer (Pierce). We immunoprecipitated Akt or CAMKKα from 750 μg protein obtained from freshly isolated whole lung homogenates using Protein A/G PLUS-Agarose beads (Santa Cruz)[29]. For immunoprecipitation, we covalently linked the antibody to Protein A/G beads as previously described[29].

Western Blot analysis

We homogenized freshly dissected lungs that we cleared from blood and BAL leukocytes in protein lysis buffer and subjected 50–75 μg of the lung lysates to Western Blot analysis[29]. We used primary and secondary antibodies following the manufacturer`s instructions. We blotted for pan-Akt, Actin or CAMKKα to assess for equal protein loading. We imaged the blots using a Kodak molecular imaging station (IS4000MM).

siRNA experiments

We purchased CAMKKα siRNA (SMARTpool siGENOME Camkk1 siRNA, Cat. # M-049735-01-0050) and Cx43 siRNA (SMARTpool siGENOME Gja1 siRNA, Cat. # M-051694-01-0005) (Thermo Scientific). For CAMKKα knockdown experiments, we intranasally instilled mice with 50 μg siRNA complexed with freshly extruded liposomes as previously described[31]. Bone marrow derived macrophages were incubated in media

containing Cx43 siRNA (2 μg/ml in lipofectamine/Opti-MEM solution) for 72 h, then treated with 1 μg/ml LPS for 24 h. We determined cytokine secretion in cell culture supernatants by ELISA. We confirmed Cx43 and CAMKKα knockdown by Western Blot.

Statistical analysis

The animals were inbred mice, hence no randomization was required. Other than survival experiments and BAL leukocyte counts, in which the investigator was blinded to mouse genotype and/or treatment, there was no blinding as animals were marked as having received LPS or buffer. All values are expressed as mean ± SEM. Data are for ≥ 10 AMs per imaging field in each experiment. We compared paired observations using paired 2-tailed Student´s *t* test or Wilcoxon rank test. We applied analysis of variance with Bonferroni´s post-hoc analysis for multiple comparisons. Mouse survival was compared using Kaplan-Meier statistics. There was no pre-specified effect size. Each experiment was replicated at least 3 times as independent biological replicates as indicated in the figure legends. Differences were considered significant at $P<0.05$.

Supplementary Material

Refer to Web version on PubMed Central for supplementary material.

Acknowledgements

We thank Dr. Boris Reizis for providing the CD11c-cre mice and Dr. Jeffrey Whitsett for providing the SPC-cre mice. We thank Dr. Ira Tabas for discussions. This study was supported by US National Institutes of Health grants HL78645, HL57556 and HL64896 to J.B., HL73989 to A.P., Parker B. Francis Fellowships to T.S.C and M.N.I.

References

1. Laskin DL, Sunil VR, Gardner CR, Laskin JD. Macrophages and tissue injury: agents of defense or destruction? Annu Rev Pharmacol Toxicol. 2011; 51:267–288. [PubMed: 20887196]
2. Medzhitov R. Toll-like receptors and innate immunity. Nat Rev Immunol. 2001; 1:135–145. [PubMed: 11905821]
3. Thorley AJ, et al. Differential regulation of cytokine release and leukocyte migration by lipopolysaccharide-stimulated primary human lung alveolar type II epithelial cells and macrophages. J Immunol. 2007; 178:463–473. [PubMed: 17182585]
4. Kuebler WM, Parthasarathi K, Wang PM, Bhattacharya J. A novel signaling mechanism between gas and blood compartments of the lung. J Clin Invest. 2000; 105:905–913. [PubMed: 10749570]
5. Maus UA, et al. Role of resident alveolar macrophages in leukocyte traffic into the alveolar air space of intact mice. Am J Physiol Lung Cell Mol Physiol. 2002; 282:L1245–L1252. [PubMed: 12003780]
6. Zhang P, Summer WR, Bagby GJ, Nelson S. Innate immunity and pulmonary host defense. Immunol Rev. 2000; 173:39–51. [PubMed: 10719666]
7. Cohen TS, Prince AS. Activation of inflammasome signaling mediates pathology of acute P. aeruginosa pneumonia. J Clin Invest. 2013; 123:1630–1637. [PubMed: 23478406]
8. Guth AM, et al. Lung environment determines unique phenotype of alveolar macrophages. Am J Physiol Lung Cell Mol Physiol. 2009; 296:L936–946. [PubMed: 19304907]
9. Caton ML, Smith-Raska MR, Reizis B. Notch-RBP-J signaling controls the homeostasis of CD8- dendritic cells in the spleen. J Exp Med. 2007; 204:1653–1664. [PubMed: 17591855]
10. Srinivas S, et al. Cre reporter strains produced by targeted insertion of EYFP and ECFP into the ROSA26 locus. BMC Dev Biol. 2001; 1:4. [PubMed: 11299042]

11. Islam MN, et al. Mitochondrial transfer from bone-marrow-derived stromal cells to pulmonary alveoli protects against acute lung injury. Nat Med. 2012; 18:759–765. [PubMed: 22504485]
12. Miller JC, et al. Deciphering the transcriptional network of the dendritic cell lineage. Nat Immunol. 2012; 13:888–899. [PubMed: 22797772]
13. Thornton EE, et al. Spatiotemporally separated antigen uptake by alveolar dendritic cells and airway presentation to T cells in the lung. J Exp Med. 2012; 209:1183–1199. [PubMed: 22585735]
14. Kirby AC, Coles MC, Kaye PM. Alveolar macrophages transport pathogens to lung draining lymph nodes. J Immunol. 2009; 183:1983–1989. [PubMed: 19620319]
15. Lindert J, Perlman CE, Parthasarathi K, Bhattacharya J. Chloride-dependent secretion of alveolar wall liquid determined by optical-sectioning microscopy. Am J Respir Cell Mol Biol. 2007; 36:688–696. [PubMed: 17290033]
16. Pfenniger A, Chanson M, Kwak BR. Connexins in atherosclerosis. Biochim Biophys Acta. 2013; 1828:157–166. [PubMed: 22609170]
17. Ichimura H, Parthasarathi K, Lindert J, Bhattacharya J. Lung surfactant secretion by interalveolar Ca2+ signaling. Am J Physiol Lung Cell Mol Physiol. 2006; 291:L596–L601. [PubMed: 16698857]
18. Wong CW, et al. Connexin37 protects against atherosclerosis by regulating monocyte adhesion. Nat Med. 2006; 12:950–954. [PubMed: 16862155]
19. Akira S, Takeda K. Toll-like receptor signalling. Nat Rev Immunol. 2004; 4:499–511. [PubMed: 15229469]
20. Li H, et al. Toll-like receptor 4-myeloid differentiation factor 88 signaling contributes to ventilator-induced lung injury in mice. Anesthesiology. 2010; 113:619–629. [PubMed: 20683250]
21. Imai Y, et al. Identification of oxidative stress and Toll-like receptor 4 signaling as a key pathway of acute lung injury. Cell. 2008; 133:235–249. [PubMed: 18423196]
22. Subramanian M, Thorp E, Hansson GK, Tabas I. Treg-mediated suppression of atherosclerosis requires MYD88 signaling in DCs. J Clin Invest. 2013; 123:179–188. [PubMed: 23257360]
23. Yano S, Tokumitsu H, Soderling TR. Calcium promotes cell survival through CaM-K kinase activation of the protein-kinase-B pathway. Nature. 1998; 396:584–587. [PubMed: 9859994]
24. Chen BC, Wu WT, Ho FM, Lin WW. Inhibition of interleukin-1beta - induced NF-kappa B activation by calcium/calmodulin-dependent protein kinase kinase occurs through Akt activation associated with interleukin-1 receptor-associated kinase phosphorylation and uncoupling of MyD88. J Biol Chem. 2002; 277:24169–24179. [PubMed: 11976320]
25. Perl AK, Wert SE, Nagy A, Lobe CG, Whitsett JA. Early restriction of peripheral and proximal cell lineages during formation of the lung. Proc Natl Acad Sci U S A. 2002; 99:10482–10487. [PubMed: 12145322]
26. Parthasarathi K, et al. Connexin 43 mediates spread of Ca2+-dependent proinflammatory responses in lung capillaries. J Clin Invest. 2006; 116:2193–2200. [PubMed: 16878174]
27. Wang L, et al. Hypoxic pulmonary vasoconstriction requires connexin 40-mediated endothelial signal conduction. J Clin Invest. 2012; 122:4218–4230. [PubMed: 23093775]
28. Decrock E, et al. IP3, a small molecule with a powerful message. Biochimica et biophysica acta. 2013; 1833:1772–1786. [PubMed: 23291251]
29. Huang BX, Kim HY. Effective identification of Akt interacting proteins by two-step chemical crosslinking, co-immunoprecipitation and mass spectrometry. PLoS One. 2013; 8:e61430. [PubMed: 23613850]
30. Centers for Disease, C & Prevention. Methicillin-resistant Staphylococcus aureus infections in correctional facilities---Georgia, California, and Texas, 2001–2003. MMWR. Morbidity and mortality weekly report. 2003; 52:992–996. [PubMed: 14561958]
31. Rowlands DJ, et al. Activation of TNFR1 ectodomain shedding by mitochondrial Ca2+ determines the severity of inflammation in mouse lung microvessels. The Journal of clinical investigation. 2011; 121:1986–1999. [PubMed: 21519143]

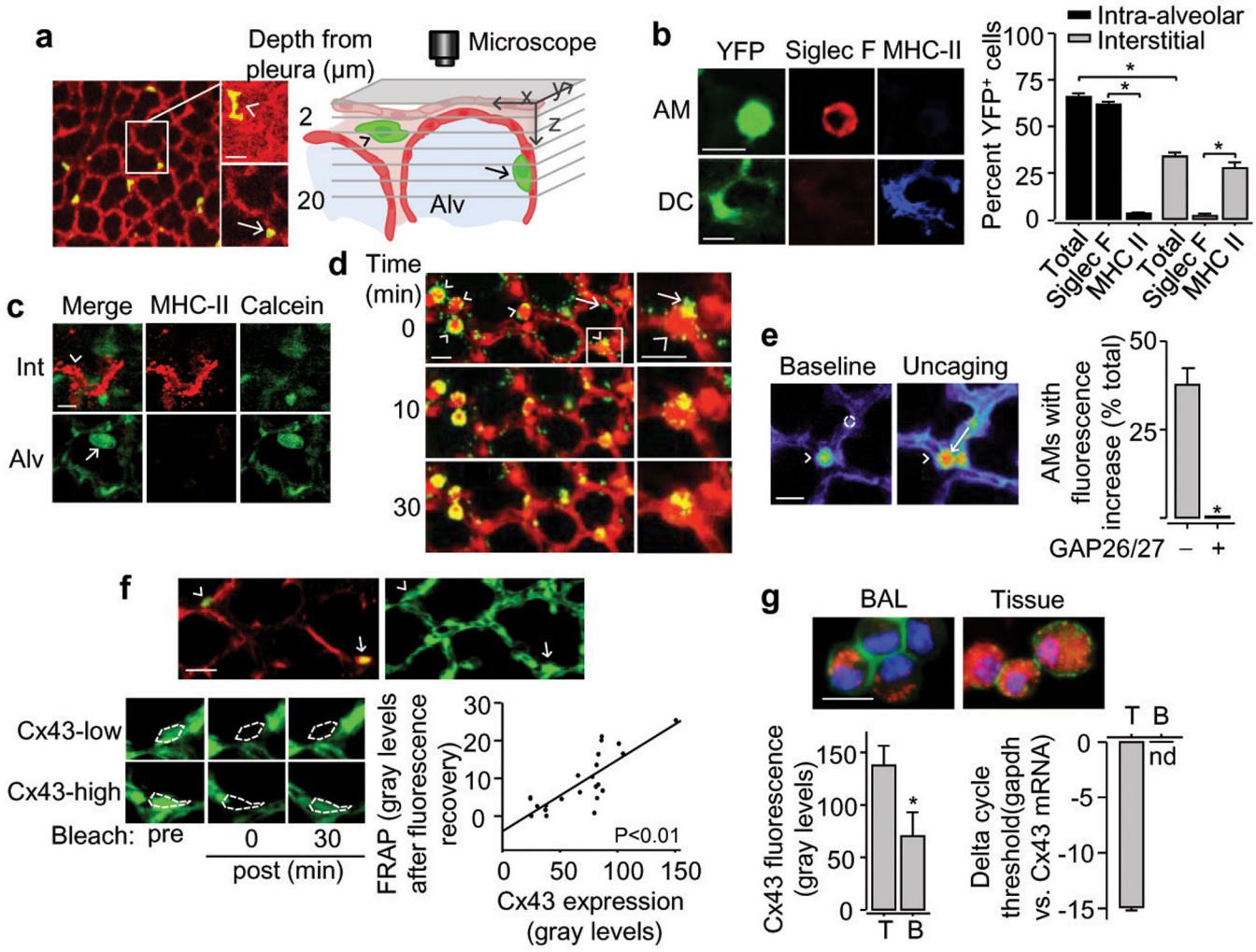

Figure 1. Live confocal microscopy of AMs *in situ*

(**a**) Interstitial (arrowhead) and luminal (arrow) YFP$^+$ cells (yellow-green) in autofluorescent alveoli (red). Sketch of imaged field. n = 15. (**b**) Immunofluorescence and quantification of alveolar (*top*) and interstitial (*bottom*) YFP$^+$ cells. n = 4 or 5. **(c)** Dye (green) injection in alveolus (Alv). Interstitial (Int) MHC-II$^+$ DC (red, arrowhead) and luminal AM (arrow). n = 3. **(d)** Merge of *S. aureus* (green, arrow in inset) with AMs (red; arrowhead in inset). n = 4 (**e**) Ca^{2+} uncaging in epithelium (dotted circle) spreads Ca^{2+} (arrow) to AM (arrowhead). Bars show GAP 26/27 effect. n = 4 or 5. (**f**) Alveoli with Cx43 (red) and calcein (green) show Cx43-low (arrowhead) and Cx43-high AMs (arrow) expressing YFP (yellow-green). High power images show calcein in AMs before (pre) and after (post) photobleaching. Line drawn by linear regression. n = 23 AMs, 4 lungs. (**g**) Cx43 (red), CD11c (green) and nuclei (blue) in AMs from BAL (B) or lung tissue (T). Bars show protein (*left*) and mRNA (*right*) expressions in AMs. n = 4.

Scale bars, 15 μm. mean±SEM. *P<0.05.

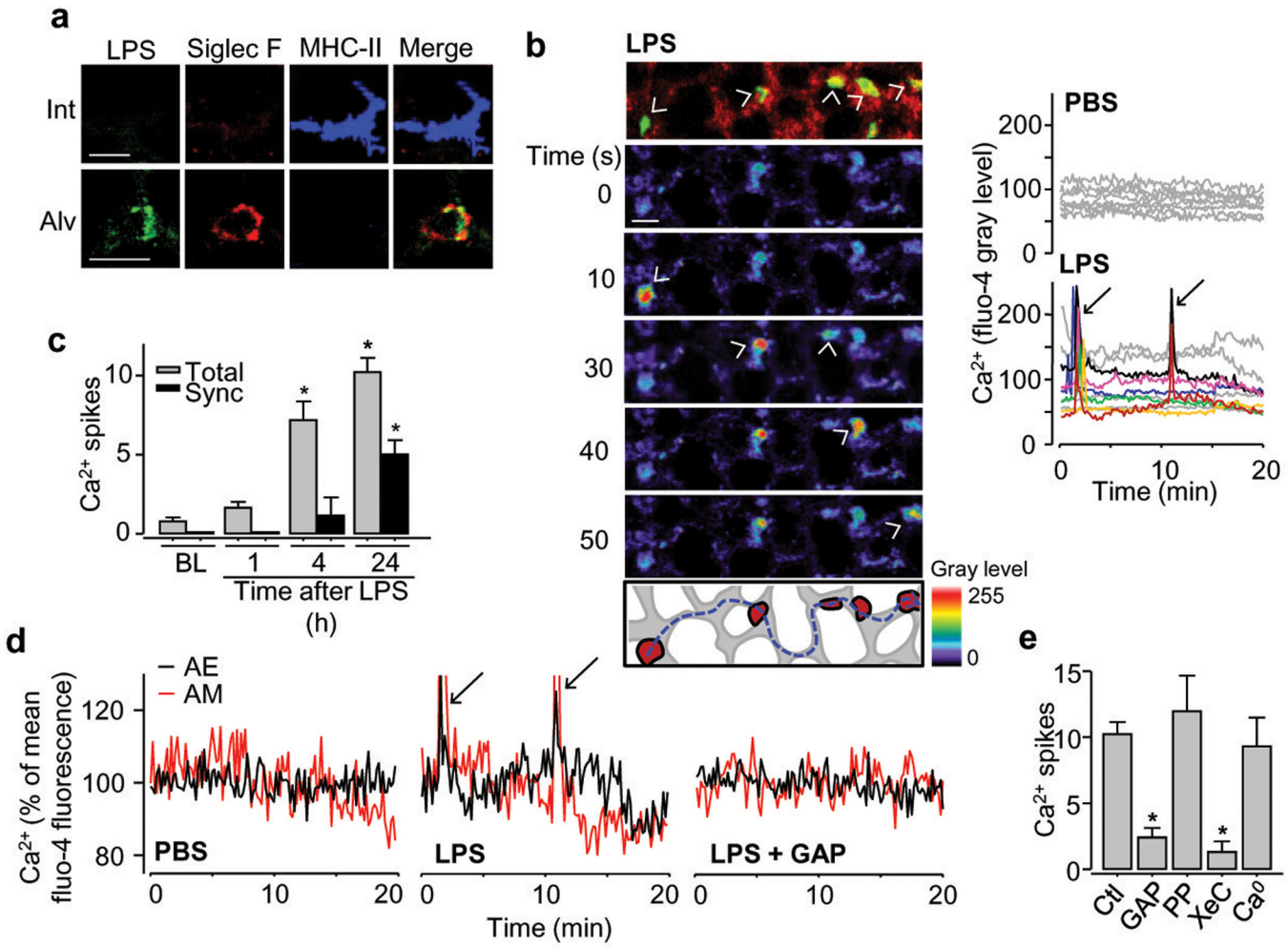

Figure 2. Communicating Ca^{2+} spikes in AMs

(**a**) Fluorescent LPS (green), AM (red) and DC (blue) in interstitium (Int) and alveolar lumen (Alv). n = 3 (**b**) YFP-expressing AMs (yellow; topmost panel), pseudocolored sequential images show increased fluo-4 fluorescence (arrowheads), 24 h after LPS. Dashes sketch spike path between AMs. Tracings show synchronous AM responses (arrows). n = 4 (**c**) Ca^{2+} spikes normalized for 10 AMs per imaging field. *Total*, all spikes; *Sync*, Synchronous spikes; *BL*, baseline (n = 8); 1h, n = 6; 4h, n = 4; 24h, n = 12 **(d)** Ca^{2+} oscillations and spikes (arrows) in AMs and adjoining alveolar epithelium (AE) 24 h after LPS or PBS. *GAP*, GAP26/27. n = 4 (**e**) Ca^{2+} spikes are 24h after LPS, normalized for 10 AMs per imaging field.*; Ctl*, LPS alone (n = 12); *PP*, PPADS (n = 4); *XeC*, xestospongin C (n = 4); Ca^{0}, Ca^{2+} depletion (n = 3). GAP, n = 5.

Scale bars, 20 μm. Bars, mean±SEM. *P<0.05 versus *Ctl* or corresponding *BL*.

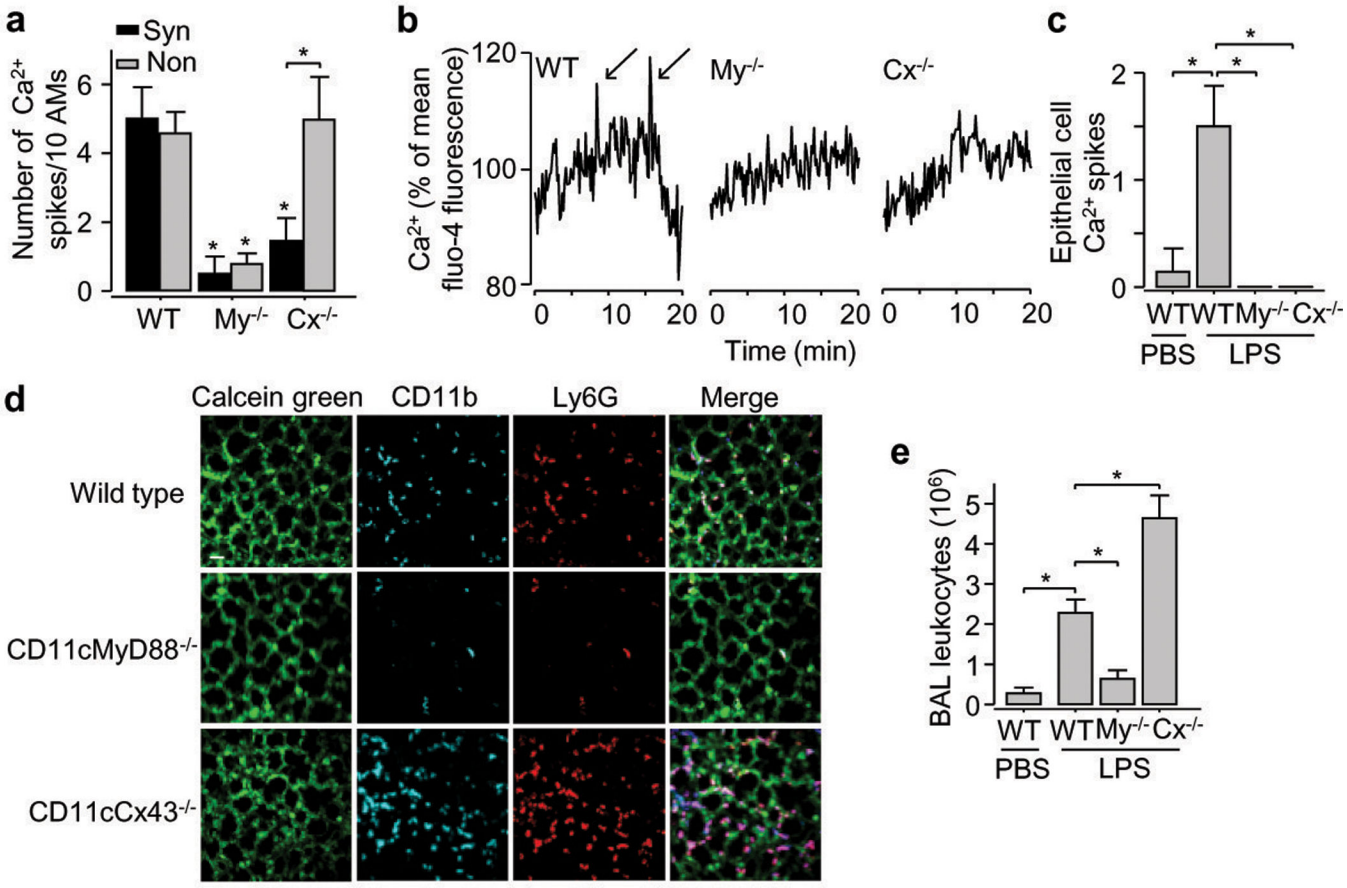

Figure 3. AM-MyD88 in inflammatory signaling

(**a-c**) Synchronized (Syn) and non-synchronized (Non) Ca^{2+} spikes (arrows) and oscillations in wild type (WT, n = 12), CD11cMyD88$^{-/-}$ ($My^{-/-}$, n = 5) and CD11cCx43$^{-/-}$ ($Cx^{-/-}$, n = 5) mice. (**d**) Alveoli (green), and $Ly6G^{+}$ (red) and $CD11b^{+}$ neutrophils (blue) 24 h after LPS. Scale bar, 30 μm. n = 4 (**e**) Responses are 24 h after treatments. LPS WT: n = 9, others: n = 4. Bars, mean±SEM. *P<0.05.

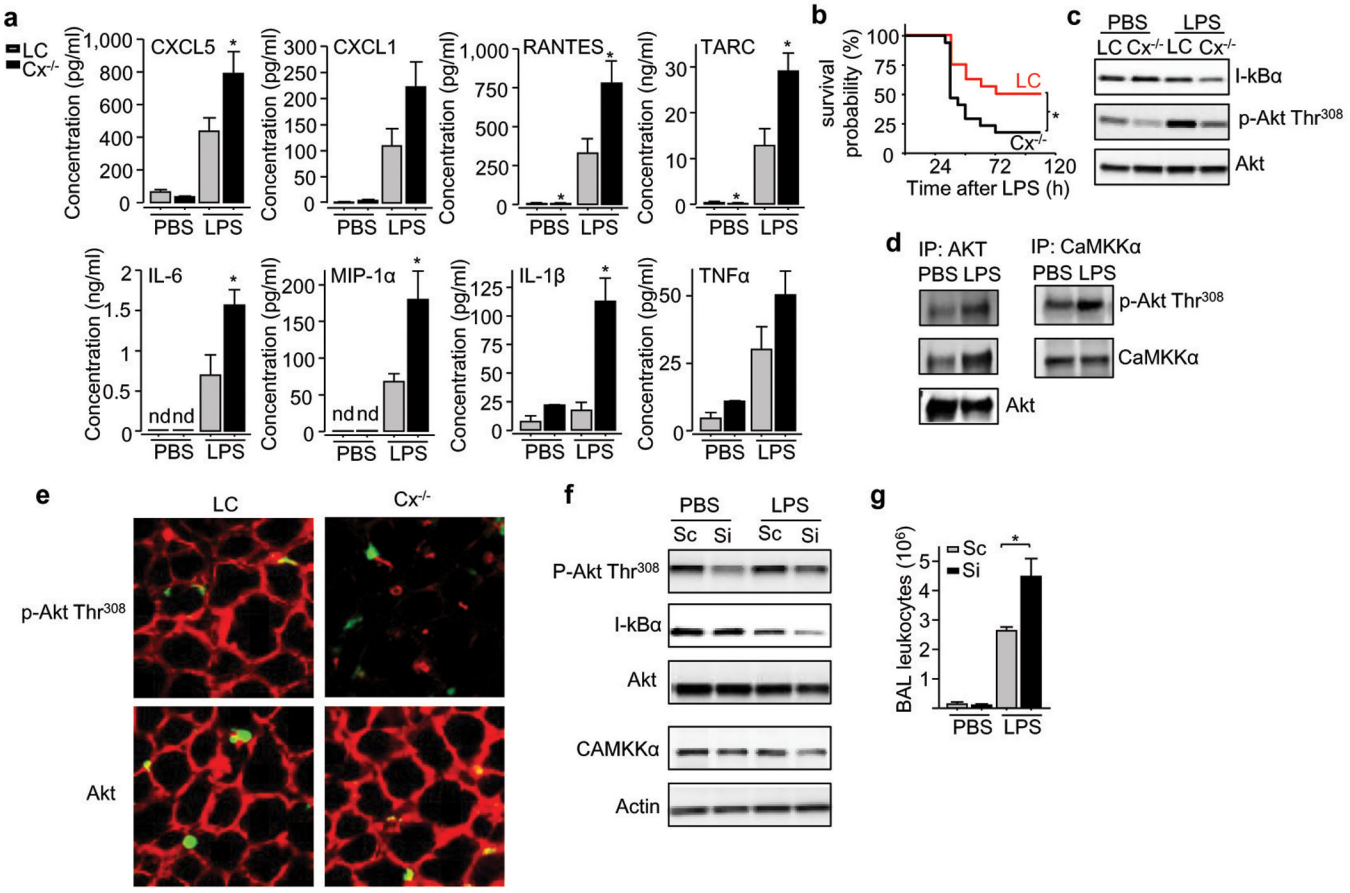

Figure 4. AM-epithelial signaling

(**a**) BAL-cytokine ELISA in CD11cCx43$^{-/-}$ (Cx$^{-/-}$) and littermate control (LC) mice. *nd*, not detectable. n = 3 or 4. (**b**) Kaplan-Meier plots. n = 16 LC, 17 Cx43$^{-/-}$. (**c,d**) Data are 24 h after treatment. IP, immunoprecipitation. n = 4 (**e**) *In situ* immunofluorescence (red) of alveolar epithelium and YFP^{+} AMs (yellow-green) 24 h after LPS. n = 4 (**f,g**) Lung lysate Western blots and BAL leukocyte counts 24 h after LPS in lungs given scrambled (Sc) or CAMKKα-specific (Si) siRNA. n = 4 for PBS+si, n = 5 for LPS+si, others: n = 6. All blots (n = 3) from same sample set. CAMKKα and Actin processed on different gel. Bars, mean ±SEM. *P<0.05.